

Discovering Strongly Correlated Quantum Spin Liquid

V. R. Shaginyan,^{1,*} K. G. Popov,² and V. A. Khodel^{3,4}

¹*Petersburg Nuclear Physics Institute, Gatchina, 188300, Russia*

²*Komi Science Center, Ural Division, RAS, Syktykar, 167982, Russia*

³*Russian Research Centre Kurchatov Institute, Moscow, 123182, Russia*

⁴*McDonnell Center for the Space Sciences & Department of Physics,
Washington University, St. Louis, MO 63130, USA*

Strongly correlated Fermi systems are among the most intriguing and fundamental systems in physics. We show that the herbertsmithite $\text{ZnCu}_3(\text{OH})_6\text{Cl}_2$ can be viewed as a new type of strongly correlated electrical insulator that possesses properties of heavy-fermion metals with one exception: it resists the flow of electric charge. We demonstrate that herbertsmithite's low temperature properties are defined by a strongly correlated quantum spin liquid made with such hypothetical particles as fermionic spinons which carry spin $1/2$ and no charge. Our calculations of its thermodynamic and relaxation properties are in good agreement with recent experimental facts and allow us to reveal their scaling behavior which strongly resembles that observed in heavy-fermion metals. Analysis of the dynamic magnetic susceptibility of strongly correlated Fermi systems suggests that there exist at least two types of its scaling.

PACS numbers: 75.40.Gb, 64.70.Tg, 76.60.Es, 71.10.Hf

Strongly correlated Fermi systems represented by heavy-fermion (HF) metals are well experimentally studied but only recently have got an adequate theoretical description [1]. Landau Fermi liquid (LFL) theory is highly successful in the condensed matter physics. The key point of this theory is the existence of fermionic quasiparticles defining the thermodynamic, relaxation and dynamic properties of conventional metals. However, strongly correlated Fermi systems encompassing a variety of systems that display behavior not easily understood within the Fermi liquid theory and called non-Fermi liquid (NFL) behavior. A paradigmatic example of the NFL behavior is demonstrated by HF metals, where a quantum phase transition (QPT) induces a transition between LFL and NFL [1, 2]. QPT can be tuned by different parameters, such as the chemical composition, the pressure, and the magnetic field. Magnetic materials, in particular insulators, are interesting subjects of study due to a quantum spin liquid (QSL) that may develop in them, defining their low-temperature properties. Exotic QSL is formed with such hypothetical particles as fermionic spinons carrying spin $1/2$ and no charge. A search for the materials is a challenge for condensed matter physics [3]. In zero and high magnetic fields B [4–13], the experimental studies of herbertsmithite $\text{ZnCu}_3(\text{OH})_6\text{Cl}_2$ have discovered gapless excitations, analogous to quasiparticle excitations near the Fermi surface in HF metals, indicating that $\text{ZnCu}_3(\text{OH})_6\text{Cl}_2$ is the promising system to investigate its QPTs and QSLs [14–16]. The observed behavior of the thermodynamic properties of $\text{ZnCu}_3(\text{OH})_6\text{Cl}_2$ strongly resembles that in HF metals since a simple kagome lattice has a dispersionless topologically protected branch of the spectrum with zero excitation energy [14, 17, 18]. This indicates that QSL formed by the ideal kagome lattice and located near the fermion

condensation quantum phase transition (FCQPT) can be considered as a strongly correlated quantum spin liquid (SCQSL). This observation allows us to establish a close connection between $\text{ZnCu}_3(\text{OH})_6\text{Cl}_2$ with its SCQSL and HF metals whose HF system is located near FCQPT and, therefore, exhibiting an universal scaling behavior [1, 14, 15]. Thus, FCQPT represents QPT of $\text{ZnCu}_3(\text{OH})_6\text{Cl}_2$ and both herbertsmithite and HF metals can be treated in the same framework, while SCQSL is composed of spinons and these with zero charge and spin $\sigma = \pm 1/2$ occupy the corresponding Fermi sphere with the Fermi momentum p_F [1, 14–16].

In our paper we show that both non-Fermi liquid and scaling behavior of such strongly correlated Fermi systems as HF metals and $\text{ZnCu}_3(\text{OH})_6\text{Cl}_2$ can be described within the frame of the theory of FCQPT. Analyzing experimental data obtained in measurements on strongly correlated Fermi systems with different microscopic properties we have found out that they demonstrate the universal non-Fermi liquid behavior. Our analysis of the dynamic magnetic susceptibility of strongly correlated Fermi systems suggests that there exist at least two types of its scaling. We calculate the thermodynamic and relaxation properties of herbertsmithite and HF metals. The calculations are in a good agreement with experimental data and allow us to detect the low-temperature behavior of $\text{ZnCu}_3(\text{OH})_6\text{Cl}_2$ defined by SCQSL as that observed in heavy fermion metals.

To study theoretically the low temperature thermodynamic, relaxation and scaling properties of herbertsmithite, we use the model of homogeneous HF liquid [1]. This model permits to avoid complications associated with the crystalline anisotropy of solids. Similar to the electronic liquid of HF metals, SCQSL is composed of chargeless fermions (spinons) with $S = 1/2$ occupy-

ing the corresponding two Fermi spheres with the Fermi momentum p_F . The ground state energy $E(n)$ is given by the Landau functional depending on the quasiparticle distribution function $n_\sigma(\mathbf{p})$, where p is the momentum and σ is the spin index. The effective mass M^* is governed by the Landau equation [1, 19]

$$\frac{1}{M^*(B, T)} = \frac{1}{M^*} + \frac{1}{p_F^2} \sum_{\sigma_1} \int \frac{\mathbf{p}_F \mathbf{p}_1}{p_F} \times F_{\sigma, \sigma_1}(\mathbf{p}_F, \mathbf{p}_1) \frac{\partial \delta n_{\sigma_1}(\mathbf{p}_1, B, T)}{\partial p_1} \frac{d\mathbf{p}_1}{(2\pi)^3}. \quad (1)$$

Here we rewrite the quasiparticle distribution function as $n_\sigma(\mathbf{p}, B, T) \equiv n_\sigma(\mathbf{p}, B = 0, T = 0) + \delta n_\sigma(\mathbf{p}, B, T)$. The Landau amplitude F is completely defined by the fact that the system has to be at FCQPT [1, 20–22], see [20–22] for details of solving Eq. (1). The sole role of Landau amplitude is to bring the system to FCQPT point, where Fermi surface alters its topology so that the effective mass acquires temperature and field dependencies. At this point, the term $1/M^*$ vanishes, Eq. (1) becomes homogeneous and can be solved analytically [1, 20]. At $B = 0$, the effective mass, being strongly T -dependent, demonstrates the NFL behavior given by Eq. (1)

$$M^*(T) \simeq a_T T^{-2/3}, \quad (2)$$

where a_T is a constant. At finite T , under the application of magnetic field B the two Fermi spheres due to the Zeeman splitting are displaced by opposite amounts, the final chemical potential μ remaining the same within corrections of order B^2 . As a result, field B drives the system to LFL region, and again it follows from Eq. (1) that

$$M^*(B) \simeq a_B B^{-2/3}, \quad (3)$$

where a_B is a constant. It is seen from Eqs. (2) and (3) that effective mass diverges at FCQPT. At finite B and T , the solutions of Eq. (1) $M^*(B, T)$ can be well approximated by a simple universal interpolating function. This interpolation occurs between the LFL regime, given by Eq. (3) and NFL regime given by Eq. (2) [1, 20]. Experimental facts and calculations show that $M^*(B, T)$ as a function of T at fixed B reaches its maximum value M_M^* at T_M , see e.g. [1]. To study the universal scaling behavior of strongly correlated Fermi system, it is convenient to introduce the normalized effective mass M_N^* and the normalized temperature T_N dividing the effective mass M^* and temperature T by their values at the maximum, M_M^* and T_M respectively. In the same way, we can normalize other thermodynamic functions such as the spin susceptibility χ and the heat capacity C . As a result, we obtain

$$\chi_N \simeq (C/T)_N \simeq M_N^*, \quad (4)$$

where χ_N and $(C/T)_N$ are the normalized values of χ and C/T , respectively. We note that our calculations of

M_N^* based on Eq. (1) do not contain any fitting parameters. The normalized effective mass $M_N^* = M^*/M_M^*$ as a function of the normalized temperature $y = T_N = T/T_M$ is given by the interpolating function [1]

$$M_N^*(y) \approx c_0 \frac{1 + c_1 y^2}{1 + c_2 y^{8/3}}. \quad (5)$$

Here $c_0 = (1 + c_2)/(1 + c_1)$, c_1 and c_2 are fitting parameters. Since magnetic field B enters Eq. (1) only in combination $B\mu_B/k_B T$, we have $T_{\max} \propto B$ [1, 20], where μ_B is the Bohr magneton and k_B is the Boltzmann constant. Thus, for finite magnetic fields variable y becomes

$$y = T/T_N \propto k_B T/\mu_B B. \quad (6)$$

Since the variables T and B enter symmetrically Eq. (5) is valid for $y = \mu_B B/k_B T$.

To construct the dynamic spin susceptibility $\chi(\mathbf{q}, \omega, T) = \chi'(\mathbf{q}, \omega, T) + i\chi''(\mathbf{q}, \omega, T)$ as a function of momentum q , frequency ω and temperature T , again we use the model of homogeneous HF liquid located near FCQPT. To deal with the dynamic properties of Fermi systems, one can use the transport equation describing a slowly varying disturbance $\delta n_\sigma(\mathbf{q}, \omega)$ of the quasiparticle distribution function $n_0(\mathbf{p})$, and $n = \delta n + n_0$. We consider the case when the disturbance is induced by the application of external magnetic field $B = B_0 + \lambda B_1(\mathbf{q}, \omega)$ with B_0 being a static field and λB_1 a ω -dependent field with $\lambda \rightarrow 0$. As long as the transferred energy $\omega < qp_F/M^* \ll \mu$, where M^* is the effective mass and μ is the chemical potential, the quasiparticle distribution function $n(\mathbf{q}, \omega)$ satisfies the transport equation [23]

$$\begin{aligned} & (\mathbf{q}\mathbf{v}_\mathbf{p} - \omega)\delta n_\sigma - \mathbf{q}\mathbf{v}_\mathbf{p} \frac{\partial n_0}{\partial \varepsilon_p} \sum_{\sigma_1 \mathbf{p}_1} f_{\sigma, \sigma_1}(\mathbf{p}\mathbf{p}_1) \delta n_{\sigma_1}(\mathbf{p}_1) \\ & = \mathbf{q}\mathbf{v}_\mathbf{p} \frac{\partial n_0}{\partial \varepsilon_p} \sigma \mu_B (B_0 + \lambda B_1). \end{aligned} \quad (7)$$

Here μ_B is the Bohr magneton and ε_p is the single-particle spectrum. In the field B_0 , the two Fermi surfaces are displaced by opposite amounts, $\pm B_0 \mu_B$, and the magnetization $\mathcal{M} = \mu_B(\delta n_+ - \delta n_-)$, where the two spin orientations with respect to the magnetic field are denoted by \pm , and $\delta n_\pm = \sum_p \delta n_\pm(\mathbf{p})$. The spin susceptibility χ is given by $\chi = \partial \mathcal{M} / \partial B|_{B=B_0}$. In fact, the transport equation (7) is reduced to two equations which can be solved for each direction \pm and allows one to calculate δn_\pm and the magnetization. The response to the application of $\lambda B_1(\mathbf{q}, \omega)$ can be found by expanding the solution of Eq. (7) in a power series with respect to $M^* \omega / qp_F$. As a result, we obtain the imaginary part of the spin susceptibility

$$\chi''(\mathbf{q}, \omega) = \mu_B^2 \frac{\omega (M^*)^2}{2\pi q} \frac{1}{(1 + F_0^q)^2}, \quad (8)$$

where F_0^a is the dimensionless spin antisymmetric quasi-particle interaction [23]. The interaction F_0^a is found to saturate at $F_0^a \simeq -0.8$ [24, 25] so that the factor $(1 + F_0^a)$ in Eq. (8) is finite and positive. It is seen from Eq. (8) that the second term is an odd function of ω . Therefore, it does not contribute to the real part χ' and forms the imaginary part χ'' . Taking into account that at relatively high frequencies $\omega \geq qp_F/M^* \ll \mu$ in the hydrodynamic approximation $\chi' \propto 1/\omega^2$ [26], we conclude that the equation

$$\chi(\mathbf{q}, \omega) = \frac{\mu_B^2}{\pi^2(1 + F_0^a)} \frac{M^* p_F}{1 + i\pi \frac{M^* \omega}{qp_F(1 + F_0^a)}}, \quad (9)$$

produces the simple approximation for the susceptibility χ and satisfies the Kramers-Kronig relation connecting the real and imaginary parts of χ .

To understand how can χ'' and χ given by Eqs. (8) and (9), respectively, depend on temperature T and magnetic field B , we recall that near FCQPT point the effective mass M^* depends on T and B . To elucidate a scaling behavior of χ , we employ Eq. (2) to describe the temperature dependence of χ . It follows from Eqs. (9) and (2) that

$$T^{2/3} \chi(T, \omega) \simeq \frac{a_1}{1 + ia_2 E}. \quad (10)$$

Here a_1 and a_2 are constants absorbing irrelevant values and $E = \omega/(k_B T)^{2/3}$. As a result, the imaginary part $\chi''(T, \omega)$ satisfies the equation

$$T^{2/3} \chi''(T, \omega) \simeq \frac{a_3 E}{1 + a_4 E^2}, \quad (11)$$

where a_3 and a_4 are constants. It is seen from Eq. (11) that $T^{2/3} \chi''(T, \omega)$ has a maximum $(T^{2/3} \chi''(T, \omega))_{\max}$ at some E_{\max} and depends on the only variable E . Equation (11) is in accordance with the scaling behavior of $\chi'' T^{0.66}$ experimentally established in Ref. [7]. As it was done for the effective mass when constructing (5), we introduce the dimensionless function $(T^{2/3} \chi'')_N = T^{2/3} \chi'' / (T^{2/3} \chi'')_{\max}$ and the dimensionless variable $E_N = E/E_{\max}$, and Eq. (11) is modified to read

$$(T^{2/3} \chi'')_N \simeq \frac{b_1 E_N}{1 + b_2 E_N^2}, \quad (12)$$

with b_1 and b_2 are fitting parameters which are to adjust the function on the right hand side of Eq. (12) to reach its maximum value 1 at $E_n = 1$.

Now we construct the schematic $T - B$ phase diagram of $\text{ZnCu}_3(\text{OH})_6\text{Cl}_2$ reported in Fig. 1. At $T = 0$ and $B = 0$ the system is near FCQPT without tuning. It can also be shifted from FCQPT by the application of magnetic field B . Magnetic field B and temperature T play the role of the control parameters, driving it from the NFL

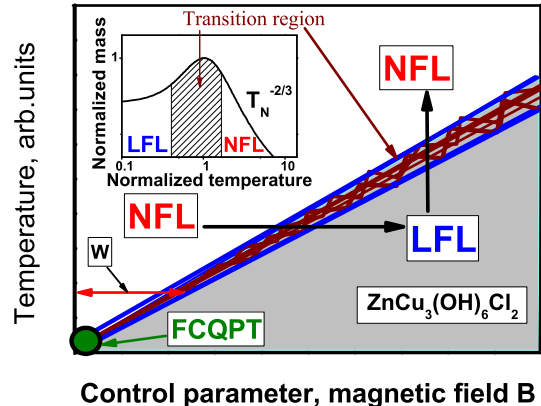


FIG. 1: (color online). Schematic $T - B$ phase diagram of $\text{ZnCu}_3(\text{OH})_6\text{Cl}_2$ located on the disordered side of FCQPT. The solid circle at the origin shown by the arrow represents FCQPT. Vertical and horizontal arrows show LFL-NFL and NFL-LFL transitions at fixed B and T respectively. The total width W of the NFL and the transition region is shown by the arrow. The inset demonstrates the behavior of the normalized effective mass M_N^* versus normalized temperature T_N as given by Eq. (5). Temperatures $T_N \sim 1$ signify a transition region between the LFL regime with almost constant effective mass and NFL one, given by $T^{-2/3}$ dependence. The transition region, where M_N^* reaches its maximum at $T/T_{\max} = 1$, is shown by the arrows and hatched area both in the main panel and in the inset.

to LFL regions as shown by the vertical and horizontal arrows. At fixed B and increasing T the system transits along the vertical arrow from the LFL region to NFL one crossing the transition region. On the contrary, at fixed T increasing B drives the system along the horizontal arrow from the NFL region to LFL one. The inset demonstrates the universal behavior of the normalized effective mass M_N^* versus normalized temperature T_N as given by Eq. (5). It follows from Eq. (5) and seen from Fig. 1 that the total width W of the NFL and the transition region, shown by the arrow in Fig. 1, tends to zero at diminishing T and B since $W \propto T \propto B$.

A few remarks are in order here. Equation (11) is valid provided that the system approaches FCQPT from the disordered side as shown in the phase diagram 1. If the system is located on the ordered side then at $B = 0$ the behavior of the effective mass as a function of T is given by [1, 28]

$$M^*(T) \simeq a_\tau T^{-1}, \quad (13)$$

where a_τ is a constant. Upon taking into account Eq. (13) and acting in the same way as it was done when deriving Eq. (11), we obtain that the imaginary part $\chi''(T, \omega)$ is given by the equation

$$T \chi''(T, \omega) \simeq \frac{a_5 E}{1 + a_6 E^2}, \quad (14)$$

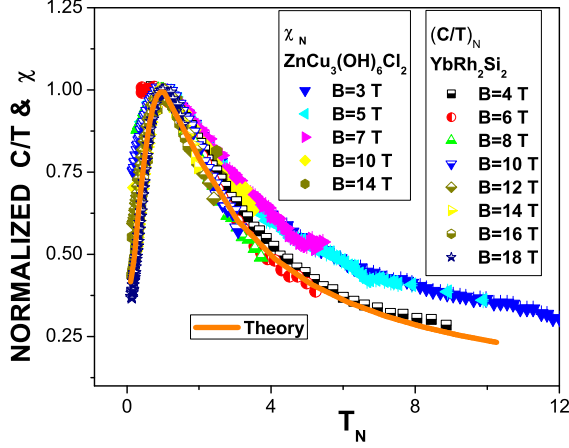


FIG. 2: (color online). The experimental data on measurements of $\chi_N \simeq (C/T)_N \simeq M_N^*$ and our calculations of M_N^* at fixed magnetic field are shown in the legends by points of different shape and solid curve respectively. It is clearly seen that the data collected on both $\text{ZnCu}_3(\text{OH})_6\text{Cl}_2$ [7] and YbRh_2Si_2 [27] merge into the same curve, obeying the scaling behavior. This demonstrates that SCQSL of herbertsmithite is close to FCQPT and behaves like HF liquid of YbRh_2Si_2 in magnetic fields.

where a_5 and a_6 are constants, and $E = \omega/k_B T$. It is seen from Eq. (14) that $T\chi''(T, \omega)$ depends on the only variable $E = \omega/k_B T$. Thus, Eqs. (11) and (14) establish two types of scaling behavior of $\chi''(\omega, T)$. Since the scaling behavior of $\chi''(\omega, T)$ is defined by the dependence of M^* on T , one may expect new types of scaling especially at the transition region shown in Fig. 1.

Figure 2 reports the behavior of the normalized χ_N and specific heat $(C/T)_N$ extracted from measurements on $\text{ZnCu}_3(\text{OH})_6\text{Cl}_2$ [7] and YbRh_2Si_2 [27], correspondingly. It follows from Fig. 2 that in accordance with Eq. (4) the behavior of χ_N coincides with that of $(C/T)_N$ in YbRh_2Si_2 .

In Fig. 3 the normalized χ_N and $(C/T)_N$, extracted from measurements on $\text{ZnCu}_3(\text{OH})_6\text{Cl}_2$ [5, 7], are depicted. To extract the specific heat C coming from the contribution of SCQSL from the total specific heat $C_t(T)$ measured on $\text{ZnCu}_3(\text{OH})_6\text{Cl}_2$, we approximate $C_t(T)$ at $T > 2$ K by the function [15]

$$C_t(T) = a_1 T^3 + a_2 T^{1/3}, \quad (15)$$

where the first term proportional to a_1 is due to the lattice (phonon) contribution and the second one is determined by SCQSL when it exhibits the NFL behavior as it follows from Eq. (2), $C \propto TM^* \propto T^{1/3}$. Taking into account that the phonon contribution is B -field independent, we obtain $C(B, T) = C_t(B, T) - a_1 T^3$. It is seen from Figs. 2 and 3 that $(C/T)_N \simeq \chi_N$ displays the same

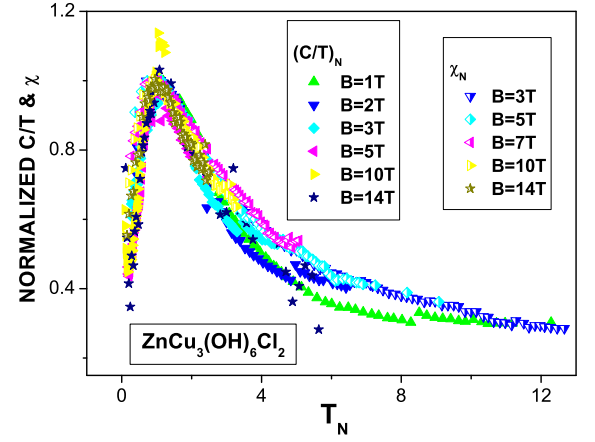


FIG. 3: (color online). The normalized susceptibility $\chi_N \simeq M_N^*$ and the normalized specific heat $(C/T)_N \simeq M_N^*$ of SCQSL versus normalized temperature T_N as a function of the magnetic fields shown in the legends. χ_N and $(C/T)_N$ are extracted from the data of [7] and [5], respectively.

scaling behavior as $(C/T)_N$ measured on the HF metal YbRh_2Si_2 . Therefore, the scaling behavior of the thermodynamic functions of herbertsmithite is the intrinsic feature of the compound and has nothing to do with magnetic impurities. The observed scaling behavior of χ_N and $(C/T)_N$ in magnetic fields shown in Figs. 2 and 3 rules out a possible supposition that extra Cu spins outside the kagome planes considered as weakly interacting impurities could be responsible for the divergent behavior of the susceptibility at low temperatures.

In Fig. 4, consistent with Eq. (12), the scaling of the normalized dynamic susceptibility $(T^{2/3}\chi'')_N$ extracted from the inelastic neutron scattering spectrum of both herbertsmithite [7], Panel A, and the HF metal $\text{Ce}_{0.925}\text{La}_{0.075}\text{Ru}_2\text{Si}_2$ [29], Panel B, is displayed. In Fig. 4, Panel C, the dynamic susceptibility $(T\chi'')$ extracted from measurements of the inelastic neutron scattering spectrum on the HF metal YbRh_2Si_2 [30] is shown. The data $(T\chi'')$ exhibit the scaling behavior over three decades of the variation of both the function and the variable, thus confirming the validity of Eq. (14). The scaled data obtained in measurements on such quite different strongly correlated systems as $\text{ZnCu}_3(\text{OH})_6\text{Cl}_2$, $\text{Ce}_{0.925}\text{La}_{0.075}\text{Ru}_2\text{Si}_2$ and YbRh_2Si_2 collapse fairly well onto a single curve over almost three decades of the scaled variables. It is seen that our calculations shown by the solid curves are in good agreement with the experimental facts. Some remarks on a role of both the disorder and the anisotropy are in order. The anisotropy is supposed to be related to the Dzyaloshinskii-Moriya interaction, exchange anisotropy, or out-of-plane impurities. Mea-

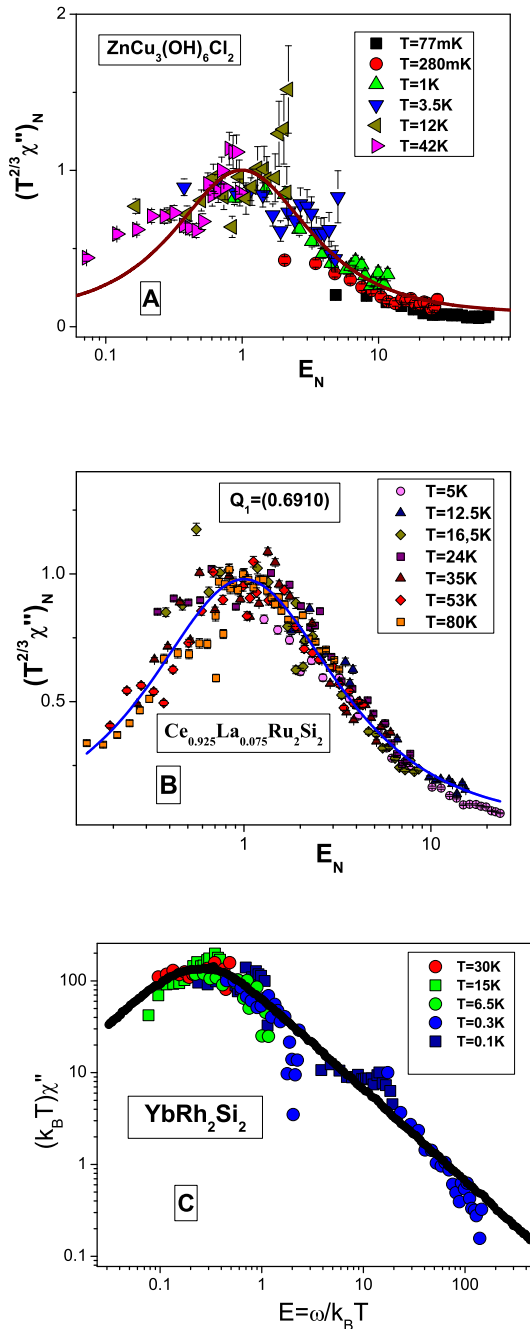


FIG. 4: (color online). Panels A and B, $(T^{2/3}\chi'')_N$ plotted against the unitless ratio $E_N = \omega/((k_B T)^{2/3} E_{\max})$. The data are extracted from measurements on ZnCu₃(OH)₆Cl₂ [7], Panel A, and Panel B, on Ce_{0.925}La_{0.075}Ru₂Si₂ obtained at Q_1 [29]. Panel C, $T\chi''$ plotted against $E = \omega/k_B T$. The data are extracted from measurements on YbRh₂Si₂ [30]. The solid curves, Panels A and B, are fits with the function given by Eq. (12), Panels C, with the function given by Eq. (14).

measurements of the susceptibility on the single crystal of

herbertsmithite have shown that it closely follows that measured on a powder sample [8, 13]. At low temperatures $T \lesssim 70$ K, the single-crystal data do not show substantial magnetic anisotropy [8, 13]. These confirm that the stoichiometry, disorder and anisotropy do not contribute significantly to the results at relatively low temperatures. As we have seen above, the scaling behavior of the thermodynamic and relaxation properties of herbertsmithite is its intrinsic feature and has nothing to do with the impurities [15]. These observations are in agreement with a general consideration of scaling behavior of HF metals [1].

In summary, we have considered the non-Fermi liquid behavior and the scaling one of such strongly correlated Fermi systems as insulator ZnCu₃(OH)₆Cl₂ and HF metals Ce_{0.925}La_{0.075}Ru₂Si₂ and YbRh₂Si₂, and shown that these are described within the frame of the theory of FCQPT. Our analysis of the dynamic magnetic susceptibility of strongly correlated Fermi systems suggests that there exist at least two types of its scaling. We calculate the thermodynamic and relaxation properties of herbertsmithite and HF metals. The calculations are in a good agreement with experimental data and allow us to identify the low-temperatures behavior of ZnCu₃(OH)₆Cl₂ determined by SCQSL as that observed in heavy fermion metals. Thus, herbertsmithite can be viewed as a new type of strongly correlated electrical insulator that possesses properties of heavy-fermion metals with one exception: it resists the flow of electric charge.

KGP acknowledges funding from the Ural Branch of the Russian Academy of Sciences, basic research program no. 12-U-1-1010, and the Presidium of the Russian Academy of Sciences, program 12-P1-1014.

* Electronic address: vrshag@thd.pnpi.spb.ru

- [1] V. R. Shaginyan, M. Ya. Amusia, A. Z. Msezane, and K. G. Popov, Phys. Rep. **492**, 31 (2010).
- [2] H.v. Löhneysen, A. Rosch, M. Vojta, and P. Wölfle, Rev. Mod. Phys. **79**, 1015 (2007).
- [3] L. Balents, Nature **464**, 199 (2010).
- [4] M. P. Shores, E. A. Nytko, B. M. Bartlett, and D. G. Nocera, J. Am. Chem. Soc. **127**, 13462 (2005).
- [5] J.S. Helton, K. Matan, M.P. Shores, E.A. Nytko, B.M. Bartlett, Y. Yoshida, Y. Takano, A. Suslov, Y. Qiu, J.-H. Chung, D.G. Nocera, and Y.S. Lee, Phys. Rev. Lett. **98**, 107204 (2007).
- [6] M. A. deVries, K. V. Kamenev, W. A. Kockelmann, J. Sanchez-Benitez, and A. Harrison Phys. Rev. Lett. **100**, 157205 (2008).
- [7] J. S. Helton, K. Matan, M. P. Shores, E. A. Nytko, B. M. Bartlett, Y. Qiu, D. G. Nocera, and Y. S. Lee, Phys. Rev. Lett. **104**, 147201 (2010).
- [8] T. H. Han, J. S. Helton, S. Chu, A. Prodi, D. K. Singh, C. Mazzoli, P. Müller, D. G. Nocera, and Y. S. Lee Phys. Rev. B **83**, 100402(R) (2011).
- [9] F. Bert and P. Mendels, J. Phys. Soc. Jpn. **79**, 011001

- (2010).
- [10] F. Mila, Phys. Rev. Lett. **81**, 2356 (1998).
- [11] S. S. Lee and P. A. Lee, Phys. Rev. Lett. **95**, 036403 (2005).
- [12] Y. Ran, M. Hermele, P. A. Lee, and X. G. Wen, Phys. Rev. Lett. **98**, 117205 (2007).
- [13] T. Han, S. Chu, and Y. S. Lee, Phys. Rev. Lett. **108**, 157202 (2012).
- [14] V. R. Shaginyan, A. Z. Msezane, and K. G. Popov, Phys. Rev. B **84**, 060401(R) (2011).
- [15] V. R. Shaginyan, A. Z. Msezane, K. G. Popov, G. S. Japaridze, and V. A. Stephanovich, Europhys. Lett. **97**, 56001 (2012).
- [16] V. R. Shaginyan, A. Z. Msezane, K. G. Popov, and V. A. Khodel, Phys. Lett. A **376**, 2622 (2012).
- [17] D. Green, L. Santos, and C. Chamon, Phys. Rev. B **82**, 075104 (2010).
- [18] T. T. Heikkila, N. B. Kopnin, and G. E. Volovik, JETP Lett. **94**, 233 (2011).
- [19] L. D. Landau, Sov. Phys. JETP **3**, 920 (1956).
- [20] J. W. Clark, V. A. Khodel, and M. V. Zverev, Phys. Rev. B **71**, 012401 (2005).
- [21] V. A. Khodel, J. W. Clark, and M. V. Zverev, Phys. Rev. B **78**, 075120 (2008).
- [22] V. R. Shaginyan, K. G. Popov, V. A. Stephanovich, V. I. Fomichev, and E. V. Kirichenko, Europhys. Lett. **93**, 17008 (2011).
- [23] D. Pines and P. Nozières, Theory of Quantum Liquids, Benjamin, New York, 1966.
- [24] M. Pfitzner and P. Wölfle, Phys. Rev. B **33**, 2003 (1986).
- [25] D. Vollhardt, P. Wölfle, and P.W. Anderson, Phys. Rev. B **35**, 6703 (1987).
- [26] D. Forster, *Hydrodynamic Fluctuations, Broken Symmetry, and Correlation Functions* (W. A. Benjamin, Inc. 1975).
- [27] P. Gegenwart, Y. Tokiwa, T. Westerkamp, F. Weickert, J. Custers, J. Ferstl, C. Krellner, C Geibel, P. Kersch, K-H. Müller, and F Steglich, New J. Phys. **8**, 171 2006.
- [28] V. A. Khodel and V. R. Shaginyan, JETP Lett. **51**, 553 (1990).
- [29] W. Knafo, S. Raymond, J. Flouquet, B. Fåk, M. A. Adams, P. Haen, F. Lapiere, S. Yates, and P. Lejay, Phys. Rev. B **70**, 174401. (2004).
- [30] C. Stock, C. Broholm, F. Demmel, J. Van Duijn, J. W. Taylor, H.J. Kang, R. Hu, and C. Petrovic, Phys. Rev. Lett. **109**, 127201 (2012).